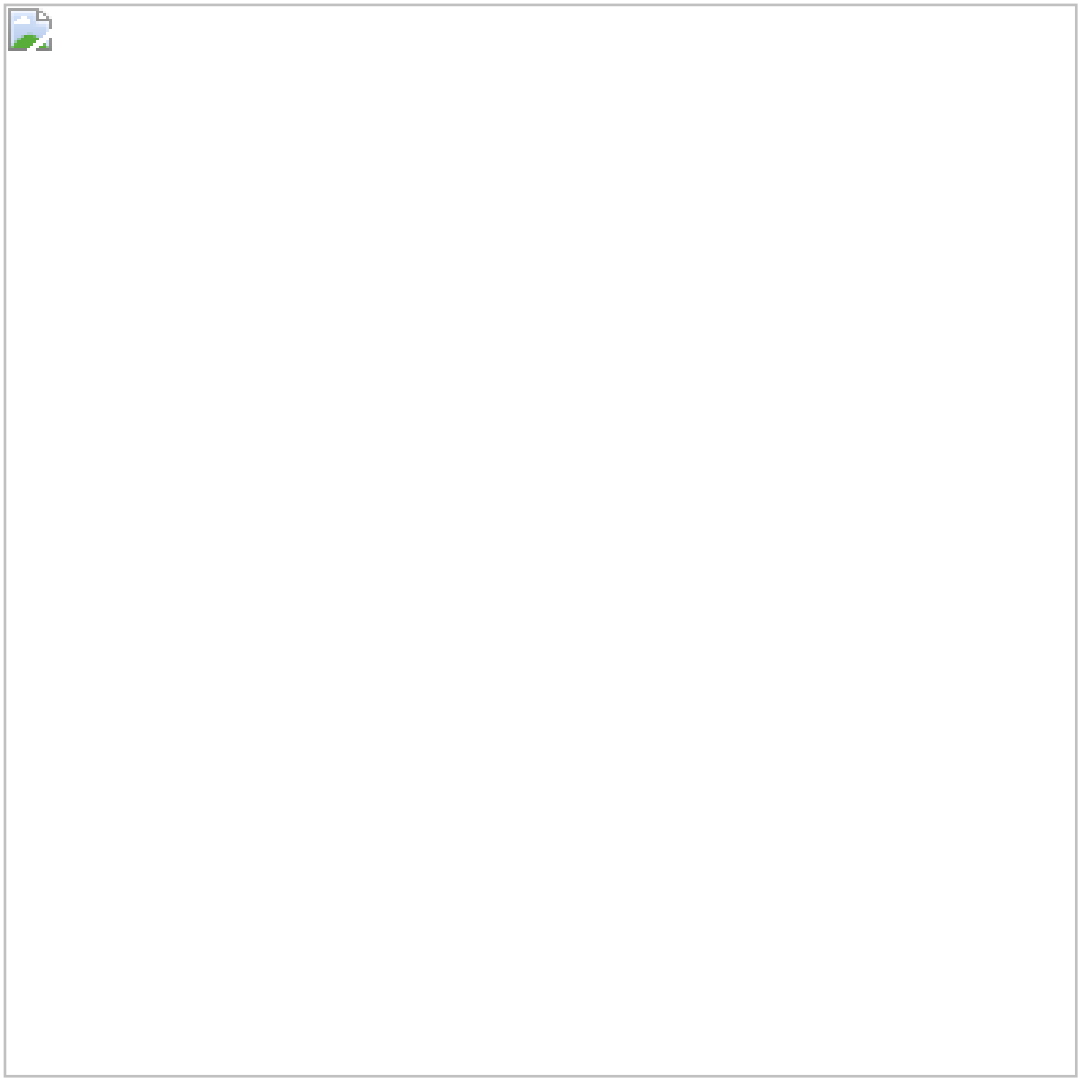

SAMiRNA Targeting Amphiregulin Alleviate Total-Body-Irradiation-Induced Renal Fibrosis

Authors: Son, Beomseok, Kim, Tae Rim, Park, Jun Hong, Yun, Sung-Il, Choi, Hanjoo, et al.

Source: Radiation Research, 197(5) : 471-479

Published By: Radiation Research Society

URL: https://doi.org/10.1667/RADE-21-00220.1

RADIATION RESEARCH **197**, 471–479 (2022)
0033-7587/22 $15.00

DOI: 10.1667/RADE-21-00220.1

SAMiRNA Targeting Amphiregulin Alleviate Total-Body-Irradiation-Induced Renal Fibrosis

Beomseok Son,[a] Tae Rim Kim,[a] Jun Hong Park,[a] Sung-Il Yun,[b] Hanjoo Choi,[a] Ji Woo Choi,[a] ChanHyeok Jeon[a] and Han-Oh Park[a,b,1]

[a] *siRNAgen Therapeutics, Daejeon 34302, Republic of Korea; and* [b] *Bioneer Corporation, Daejeon 34302, Republic of Korea*

Son B, Kim TR, Park JH, Yun S-I, Choi H, Choi JW, Jeon C, Park H-O. SAMiRNA Targeting Amphiregulin Alleviate Total-Body-Irradiation-Induced Renal Fibrosis. Radiat Res. 197, 471–479 (2022).

Fibrosis is a serious unintended side effect of radiation therapy. In this study, we aimed to investigate whether amphiregulin (AREG) plays a critical role in fibrosis development after total-body irradiation (TBI). We found that the expression of AREG and fibrotic markers, such as α-smooth muscle actin (α-SMA) and collagen type I alpha 1 (COL1α1), was elevated in the kidneys of 6 Gy TBI mice. Expression of AREG and α-SMA was mainly elevated in the proximal and distal tubules of the kidney in response to TBI, which was confirmed by immunofluorescence staining. Knockdown of *Areg* mRNA using self-assembled-micelle inhibitory RNA (SAMiRNA) significantly reduced the expression of fibrotic markers, including α-SMA and COL1α1, and inflammatory regulators. Finally, intravenous injections of SAMiRNA targeting mouse *Areg* mRNA (SAMiRNA-mAREG) diminished radiation-induced collagen accumulation in the renal cortex and medulla. Taken together, the results of the present study suggest that blocking of AREG signaling via SAMiRNA-mAREG treatment could be a promising therapeutic approach to alleviate radiation-induced kidney fibrosis.

INTRODUCTION

Even though various classes of anticancer drugs are available, 60% of cancer patients receive radiation therapy. High-energy radiation, such as X and γ rays can cause serious damage to cancer cells, regardless of whether they are drug-resistant or not. However, this procedure inevitably affects normal cells in the tumor environment (*1*). X and γ rays are categorized as ionizing radiation and reportedly induce atom ionization causing serious cellular damage, including DNA damage, lipid peroxidation, and protein oxidation (*2*). In humans, exposure to radiation doses higher than 0.5 Gy leads to acute radiation syndrome (ARS), including hematopoietic, gastrointestinal, and neurovascular sub-syndromes (*3*). Therefore, animal models of ARS have been developed to identify effective drugs to alleviate ARS-associated symptoms (*3–6*). On the other hand, several previous clinical and preclinical studies applying bone marrow transfusion suggested that total-body irradiation (TBI) induced late biological effects, such as pulmonary and cardiac fibrosis, renal dysfunction, malfunction of the immune system, and tumorigenesis (*7–11*).

Amphiregulin (AREG) is an epidermal growth factor receptor (EGFR) ligand synthesized as a transmembrane precursor. Its activation occurs via juxtacrine signaling during wound healing and fibrotic processes (*12*), after which AREG is generated from pro-AREG by disintegrin and metalloproteinase (ADAM) 17-mediated cleavage. This results in the release of a mature EGFR ligand, which is known to act in an autocrine, paracrine, or endocrine fashion (*12, 13*). Previous studies have focused on the role of AREG in managing inflammation and tissue repair (*14–16*). AREG is also known to be involved in fibrotic tissue formation mediated by transforming growth factor-β1 (TGF-β1), as uncontrolled and exaggerated wound healing processes can lead to tissue fibrosis (*17–21*). Importantly, *AREG* silencing using small interfering RNA (siRNA) is sufficient to inhibit fibroblast proliferation and to reduce collagen accumulation in the lungs of TGF-β1 transgenic mice (*22*).

The role of AREG in TBI-mediated processes has not been studied extensively in the past. Shao et al. suggested that AREG plays a critical role in intestinal epithelial growth after 12 Gy TBI. Accordingly, expression of *Areg* messenger (m)RNA was elevated in the intestines of C57BL/6 mice after irradiation, whereas that of other EGFR ligands, including *Egf* and *Tgfa* mRNAs, was not significantly altered (*23*). However, whether AREG function is linked to radiation-induced wound healing processes or fibrosis is yet to be investigated. We thus aimed to investigate the changes in AREG expression in different

Editor's note. The online version of this article (DOI: https://doi.org/10.1667/RADE-21-00220.1) contains supplementary information that is available to all authorized users.

[1] Address for correspondence: Han-Oh Park, siRNAgen Therapeutics and Bioneer Corporation, 8-11 Munpyeongseo-ro, Daedeok-gu, Daejeon 34302, Republic of Korea: email: hpark@bioneer.com.

organs after TBI, as well as the role of AREG in radiation-induced fibrosis.

RNA interference (RNAi) technology is employed to inhibit translation of mRNAs into proteins using complementary sequences to certain mRNA segments (*24*). By targeting key proteins involved in disease development, nanomedicine-based approaches employing RNAi technology are considered emerging therapeutic strategies (*25*). However, unintended innate immune stimulation and off-target effects are challenges to RNAi-based approaches (*26, 27*). To overcome these limitations, we developed a novel siRNA modality conjugated with a hydrophobic hydrocarbon and hydrophilic polymer at the 5′ and 3′ ends of the siRNA sense strand, respectively. As the modified siRNA molecules form micelles in physiological solution without any additives or processing steps, they are referred to as self-assembled-micelle inhibitory RNA (SAMiRNA). In contrast to naked siRNA or encapsulated liposomes, SAMiRNA was shown not to elicit innate immune responses (*19*). Moreover, SAMiRNA targeting mouse *Areg* mRNA (SAMiRNA-mAREG) inhibited the expression of *Areg* mRNA and alleviated pulmonary or renal fibrosis development upon successful delivery to target organs (*19, 28*).

Several previous studies utilized RNAi technology to alleviate radiation-induced organ damage. Knockdown of *Apc* mRNA, which is a negative regulator of Wnt, resulted in Wnt pathway activation and mitigation of gastrointestinal syndrome induced by whole-abdomen irradiation (*29*). Delivery of TGF-β1 or Smad3 siRNA to the lungs or skin, respectively, reduced radiation-induced injuries (*30, 31*). Regulating expression of specific genes involved in radiation response or fibrosis development has recently gained increasing research interest (*32, 33*).

The current study was conducted to investigate whether SAMiRNA-mAREG is applicable to radiation-induced fibrosis treatment. For this, mRNA expression levels of *Areg* and fibrosis markers were measured in various organs at different time points after TBI. We also examined possible correlations between AREG and fibrotic marker expression levels using intravenous (i.v.) injection of SAMiRNA-mAREG in 6 Gy TBI mice. After administration of SAMiRNA-mAREG, we investigated the expression levels of AREG and α-smooth muscle actin (α-SMA), as well as collagen deposition. We examined the role of AREG in TBI-induced fibrosis and the potential of SAMiRNA-mAREG as a novel therapeutic agent for the treatment of radiation-induced kidney fibrosis.

MATERIALS AND METHODS

Animal Experiments and Irradiation

All experimental methods and protocols were approved by the Committee on the Ethics of Animal Experiments of the siRNAgen Therapeutics Corporation (Daejeon, Republic of Korea, siRNAgen Therapeutics IACUC, AEC-20200319-0002). The siRNAgen Therapeutics-IACUC was approved by the Animal and Plant Quarantine Agency (Gimcheon-si, Gyeongsangbuk-do, Republic of Korea). We used 7-week-old male C57BL/6 mice for the TBI studies, which were maintained in individual cages. Five mice were included in each experimental group. Single-dose TBI at a dose rate of 1 Gy/min was performed using a Gammacell 3000 Elan irradiator (Nordion, Canada) provided by the KAIST Analysis Center for Research Advancement (KARA) at the Korea Advanced Institute of Science and Technology (KAIST, Daejeon, Republic of Korea). The mice were euthanized at the times indicated, after which the organs were harvested for quantitative reverse transcription (qRT)-PCR and histological analyses.

SAMiRNA Design and Treatment

SAMiRNA was manufactured as described previously (*19*). SAMiRNA-mAREG (30 mg/mL) was diluted to a final concentration of 5 mg/kg for injections using Dulbecco's phosphate-buffered saline (DPBS; Welgene, Gyeongsan, Republic of Korea). The molecular weights of the SAMiRNA-mAREG sense and antisense strands were measured using the Axima LNR MALDI-TOF MS system (Kratos Analytical, Shimadzu, UK). The purity of SAMiRNA-mAREG single strand preparations was analyzed by high-performance liquid chromatography (Shimadzu, Kyoto, Japan), and was determined to be ≥40% of sense and antisense strands, respectively. The osmolality of SAMiRNA-mAREG was in the range of 320 ± 30 mOsmol/kg, which was measured using an Osmomat 3000 (Gonotec, Berlin, Germany). The size of SAMiRNA-mAREG was analyzed using Zetasizer Nano-ZS (Malvern Panalytical, UK) and qNano Gold instruments (Izon Science Ltd., Christchurch, New Zealand), which was determined to be ≤200 nm. For 6 Gy TBI experiments, SAMiRNA-mAREG at 5 mg/kg in 100 μL of DPBS or 100 μL of DPBS were administered intravenously biweekly (from weeks 4 to 12 after TBI) or weekly (from weeks 13 to 23 after TBI) via the tail veins of the mice. The dosing schedule was determined on the basis of results from 4 Gy TBI experiments and weeks 4 and 8 after TBI of 6 Gy models.

qRT-PCR

Total RNA was extracted using the AccuPrep Universal RNA Extraction Kit (Bioneer, Daejeon, Republic of Korea) or the AccuPrep Blood RNA Extraction Kit (Bioneer) according to the manufacturer's protocol. After determining the RNA concentration based on the absorbance at 260 nm (Tecan, Groedig, Austria), cDNA was synthesized from 1 μg of total RNA using the AccuPower RocketScript Cycle RT PreMix (Bioneer) and AllInOneCycler PCR system (Bioneer). AccuPower 2× GreenStar qPCR MasterMix (Bioneer) and an Exicycler 96 (Bioneer) were employed to quantify cDNA targets. Expression levels of mRNAs encoding fibrotic markers, inflammatory regulators, and reference genes were quantitatively analyzed using qRT-PCR. Primer sequences are listed in Supplementary Table S1 (https://doi.org/10.1667/RADE- 21-00220.1.S1). β-actin (*Actb*) and hypoxanthine phosphoribosyltransferase 1 (*Hprt*) were used as housekeeping genes. Data were analyzed using the $2^{-\Delta\Delta Ct}$ method.

Immunofluorescence (IF) Staining

Paraffin-embedded tissue sections were deparaffinized, submerged in 1 mM ethylenediaminetetraacetic acid at pH 8.0 and 90°C, and allowed to cool for 30 min for antigen retrieval. The sections were incubated in 0.3% Triton X-100 in PBS for 5 min at 20°C for permeabilization. Nonspecific antibody-binding sites were blocked with 5% normal goat serum (Cell Signaling Technology, Danvers, MA) in PBS for 30 min at 20 °C. Next, fluorescence-conjugated anti-AREG and anti-α-SMA primary antibodies (Santa Cruz Biotechnology, Santa Cruz, CA; 1:200 dilutions) were added to the tissue sections, which were subsequently incubated for 16 h at 4°C. After three sequential washing steps with PBS, the tissue sections were mounted with Vectashield mounting medium containing 4′,6-diamidino-2-phenylindole (DAPI; Vector Laboratories Burlingame,

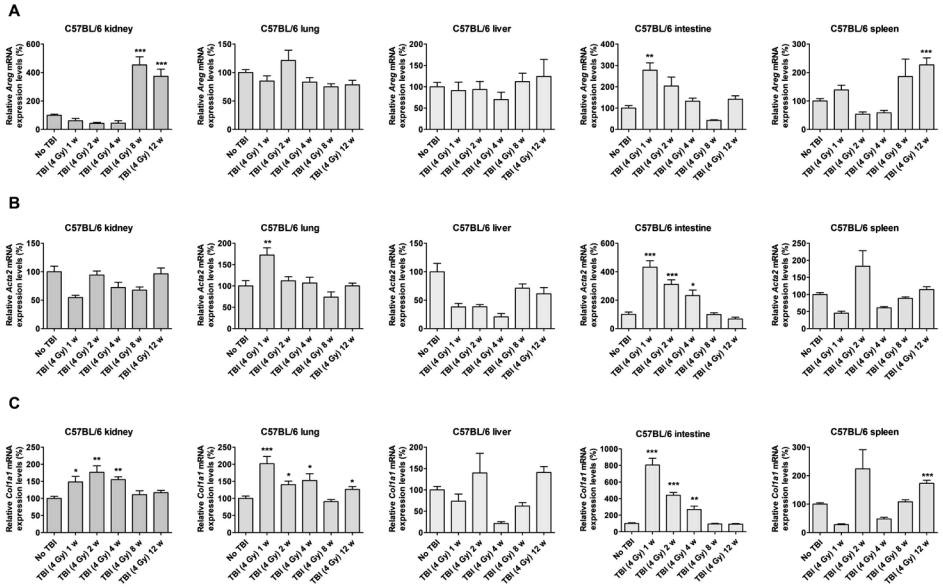

FIG. 1. Gene expression analysis of the kidney, lung, liver, intestine, and spleen of a 4 Gy total-body irradiation (TBI) mouse model. Panel A: Amphiregulin (*Areg*) expression in the kidney, lung, liver, intestine, and spleen of C57BL/6 mice subjected to 4 Gy TBI was examined by quantitative reverse transcription (qRT)-PCR. Panels B and C: Expression levels of the fibrosis markers α-smooth muscle actin (*Acta2*) and collagen type I alpha 1 (*Col1a1*) were evaluated in various organs isolated from 4 Gy TBI model mice. Relative expression levels were calculated for each time point, with the values obtained using non-irradiated mice set to 100. For quantifications, data (mean ± SEM) were analyzed by t-tests. $^{*}p < 0.05$, $^{**}p < 0.01$, and $^{***}p < 0.001$ compared to non-irradiated mice.

CA). Confocal laser scanning images were obtained using a Dragonfly confocal microscopy system (Andor, Belfast, Northern Ireland).

Masson's Trichrome Staining

Kidney tissues were fixed in 10% neutral-buffered formalin and embedded in paraffin. The samples were then sectioned and subjected to Masson's trichrome staining to detect collagen fibers following standard procedures. Images were acquired using a Nikon Eclipse Ts2 microscope (Nikon, Tokyo, Japan). Fibrotic areas were quantified by measuring the blue areas using Fiji software (*45*).

Measurements of BUN and sCr Levels

To measure BUN and sCr levels, whole blood was collected in BD Microtainer blood collection tubes (BD Biosciences, Franklin Lakes, NJ) as the mice were sacrificed, and blood samples were incubated at 20°C for 15 min to promote clotting. Whole blood samples were then centrifuged at 3,000 rpm and 4°C for 10 min, and the supernatants were used to measure BUN and sCr levels using an automatic analyzer (Hitachi 7180; Hitachi High-Technologies Co., Tokyo, Japan).

Statistical Analysis

Data are expressed as mean ± standard error of the mean (SEM). The results were statistically analyzed by t-tests. Differences were considered significant at a $p < 0.05$.

RESULTS

Fibrotic Phenotypes are not Induced at 12 Weeks after 4 Gy TBI

Previous reports have suggested that fibrosis could develop in several organs as a side effect of radiation therapy or in irradiated experimental animals (*7, 34, 35*). To determine the molecular mechanisms of radiation-induced fibrosis and to develop potential treatment strategies, we initially used 4 Gy TBI to establish a fibrosis model using C57BL/6 mice. Based on this model, we investigated *Areg*, *Acta2*, and *Col1a1* expression in various organs at 1, 2, 4, 8, and 12 weeks after 4 Gy TBI (Fig. 1). *Areg* expression was increased in the kidney, intestine, and spleen at 8 and 12, 1, and 12 weeks after 4 Gy TBI, respectively (Fig. 1A). However, increased *Acta2* and *Col1a1* expression was not observed in the kidney, lung, liver, intestine, and spleen at 12 weeks after 4 Gy TBI (Fig. 1B and C). Moreover, we discovered that the basal mRNA expression level of *Areg* was very low in the heart, blood, and bone marrow of C57BL/6 mice. Collectively, these data suggest that 4 Gy TBI led to increased *Areg* expression levels in the kidney, intestine, and spleen, which did not lead to fibrosis formation in C57BL/6 mice.

Kidney Fibrosis and Inflammation Develop at 24 weeks after 6 Gy TBI and can be Inhibited by SAMiRNA-mAREG Treatment

Following gene expression analysis after 4 Gy TBI, we investigated whether an elevated dose (6 Gy) and an extended post-TBI period (24 weeks) could elicit fibrosis in C57BL/6 mice. *Areg* expression in the kidney was elevated at 4, 8, 12, and 16 weeks after 6 Gy TBI, but the expression of *Tgfb1*, which leads to reciprocal activation of AREG signaling (*16, 17*), and fibrosis markers was not increased

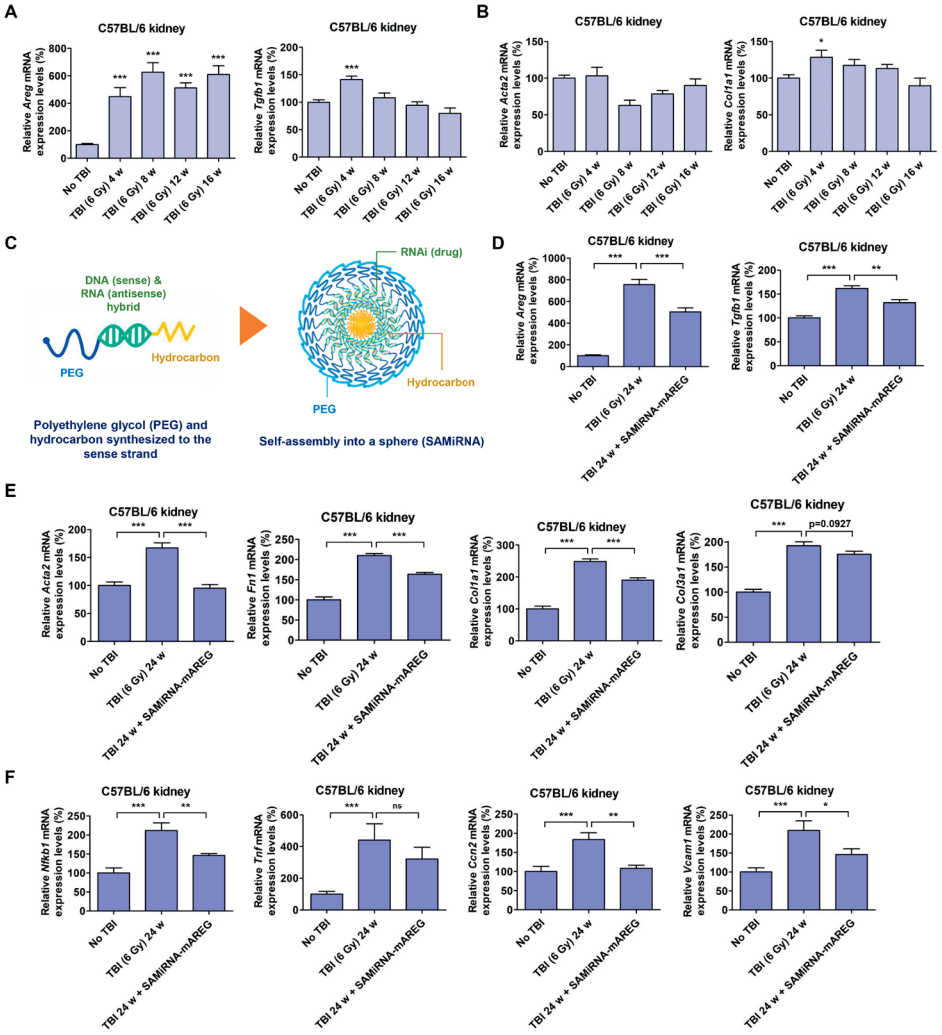

FIG. 2. Expression of renal fibrosis and inflammation markers is induced at 24 weeks after 6 Gy total-body irradiation (TBI), which can be attenuated by self-assembled-micelle inhibitory RNA targeting mouse amphiregulin mRNA (SAMiRNA-mAREG) injection. Panels A and B: Renal expression levels of *Areg*, transforming growth factor-β1 (*Tgfb1*), α-smooth muscle actin (*Acta2*), and collagen type I alpha 1 (*Col1a1*) were analyzed by quantitative reverse transcription (qRT)-PCR at 4, 8, 12, and 16 weeks after 6 Gy TBI. $^{*}p < 0.05$ and $^{***}p < 0.001$ compared to non-irradiated mice. Panel C: A graphic of self-assembled-micelle inhibitory RNA (SAMiRNA) structure. Panels D-F: At 24 weeks post-TBI, expression levels of *Areg*, *Tgfb1*, fibrosis-related genes (*Acta2*, *Fn1*, *Col1a1*, and *Col3a1*), and inflammation regulators (nuclear factor-κB subunit 1; *Nfkb1*, tumor necrosis factor-α; *Tnf*, connective tissue growth factor; *Ccn2*, and vascular cell adhesion molecule 1; *Vcam1*) after TBI with or without SAMiRNA-mAREG treatment were analyzed by qRT-PCR. $^{*}p < 0.05$, $^{**}p < 0.01$, and $^{***}p < 0.001$ compared to non-irradiated or TBI-only mice. Expression of *Tnf* was not significantly (ns) reduced by SAMiRNA-mAREG treatments due to large variation between mice in the same group. Relative gene expression levels were calculated for each time point, with the values obtained using non-irradiated mice set to 100. For quantifications, data (mean ± SEM) were analyzed by t-tests.

(Fig. 2A and B). However, we found that the expression levels of *Areg* and *Tgfb1* were increased at 24 weeks after 6 Gy TBI (Fig. 2D). Furthermore, expression of the fibrotic markers, *Acta2*, *Fn1*, *Col1a1*, and *Col3a1* was also increased at 24 weeks (Fig. 2E). Taken together, these results suggest that kidney fibrosis had developed over the course of 24 weeks in response to 6 Gy TBI.

Our previous studies demonstrated that SAMiRNA-mAREG, the structure of which is depicted in Fig. 2C, exert therapeutic effects on pulmonary fibrosis induced by bleomycin or in TGF-β-transgenic mice, as well as on UUO- or adenine diet-induced renal fibrosis and inflammation (*19, 28*). Therefore, we analyzed the effects of SAMiRNA-mAREG on TBI-induced renal fibrosis and inflammation. TBI-dependent upregulation of *Areg* expression was significantly inhibited by SAMiRNA-mAREG treatment, and *Tgfb1* expression was concomitantly decreased (Fig. 2D). We also confirmed that SAMiRNA-mAREG inhibited TBI-induced *Acta2*, *Fn1*, *Col1a1*, and *Col3a1* expression (Fig. 2E). Overexpression of inflammatory mediators such as *Nfkb1*, *Tnf*, *Ccn2*, and *Vcam1* was induced by TBI, which was reversed by SAMiRNA-

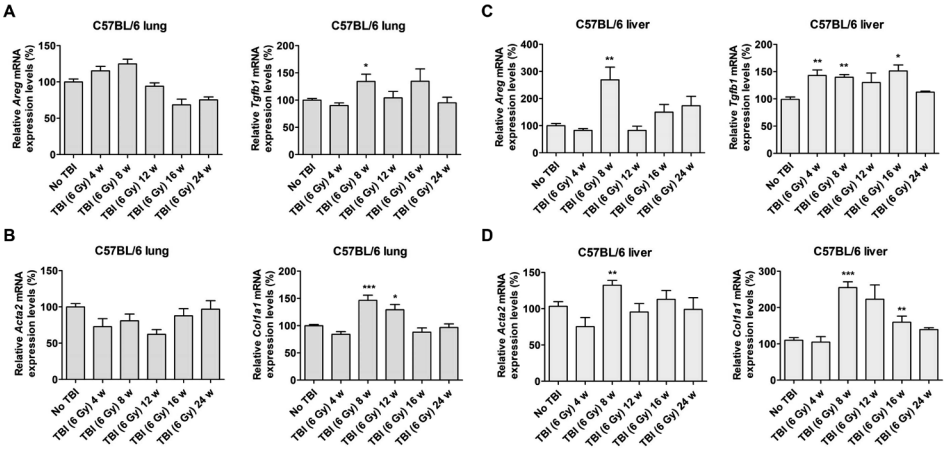

FIG. 3. No significant activation of amphiregulin (AREG) signaling and fibrosis development is observed in the lung and liver of 6 Gy total-body irradiation (TBI) model mice. Panels A and B: Expression levels of *Areg*, transforming growth factor-β1 (*Tgfb1*), α-smooth muscle actin (*Acta2*), and collagen type I alpha 1 (*Col1a1*) in the lung at 24 weeks post-TBI. Panels C and D: mRNA expression levels of AREG signaling components and fibrosis markers in the liver of 6 Gy TBI model mice were assessed by quantitative reverse transcription (qRT)-PCR. Relative expression levels were calculated for each time point, with the values obtained using non-irradiated mice set to 100. For quantifications, data (mean ± SEM) were analyzed by t-tests. $^{*}p < 0.05$, $^{**}p < 0.01$, and $^{***}p < 0.001$ compared to non-irradiated mice.

mAREG (Fig. 2F). Expression of *Il1b* and *Icam1*, which are other inflammatory markers, was not increased by TBI (Supplementary Fig. S1; https://doi.org/10.1667/RADE-21-00220.1.S1), and that of *Il10*, *Il17a*, and *Ifng* in the kidneys was very low. These results demonstrated that i.v. injection of SAMiRNA-mAREG ameliorated renal fibrosis and inflammation induced by 6 Gy TBI via knockdown of *Areg* expression.

Fibrosis is not Induced in the Lung, Liver, Intestine, and Spleen at 24 Weeks after 6 Gy TBI

After fibrosis formation in the kidney in response to 6 Gy TBI had been confirmed, we also evaluated *Areg* and fibrosis marker expression levels in the lung, liver, intestine, and spleen. The pulmonary expression levels of *Tgfb1* and *Col1a1* were increased at 8 weeks after TBI, but the observed overexpression was not sustained at later time points (Fig. 3A and B). In the lung, *Areg* or *Acta2* overexpression after TBI was not observed at any of the time points analyzed. In the liver, upregulation of *Areg* and fibrosis marker expression was detected at 8 weeks after 6 Gy TBI (Fig. 3C and D). However, *Areg*, *Tgfb1*, *Acta2*, and *Col1a1* expression was not increased in the liver of 6 Gy TBI mice compared to non-irradiated mice at 24 weeks after TBI.

In accordance with a previous report (*23*), *Areg* expression in the intestine was increased by TBI at an early time point (Fig. 4A). Nonetheless, expression levels of *Acta2* and *Col1a1* in the intestine were not significantly elevated by 6 Gy TBI at the times analyzed (Fig. 4B). Although *Areg* expression was increased in the spleen at 16 and 24 weeks after TBI, fibrosis was not detected at 24 weeks after TBI (Fig. 4C and D). These results suggest that 6 Gy TBI C57BL/6 mice did not lead to fibrosis formation in the lung, liver, intestine, and spleen at 24 weeks postirradiation.

SAMiRNA-mAREG Treatment Attenuates 6 Gy TBI-Induced AREG and α-SMA Protein Expression and Collagen Deposition in the Kidney

After confirming the overexpression of mRNAs encoding AREG and fibrosis markers in the kidney in response to TBI, we assessed the protein levels and localization of AREG and α-SMA by IF staining. The results showed that the expression of AREG and α-SMA proteins was upregulated by 6 Gy TBI. Moreover, the proteins were found to be predominantly expressed in the proximal and distal tubules of the kidney (Fig. 5A). We also confirmed that i.v. injection of SAMiRNA-mAREG inhibited overexpression of AREG and α-SMA at the protein level (Fig. 5A and B).

Masson's trichrome staining is widely used to characterize renal fibrosis formation and to verify the deposition of collagen, which stains blue (*28*). As shown in Fig. 6A, the kidneys of TBI mice displayed significant interstitial collagen deposition compared to those of non-irradiated control mice. Masson's trichrome staining also revealed that SAMiRNA-mAREG treatment reduced the TBI-induced collagen deposition (Fig. 6A and B). Collectively, these results demonstrated that SAMiRNA-mAREG treatment led to reduced AREG and α-SMA protein expression and collagen deposition in the kidneys of 6 Gy TBI mice.

Kidney Function is not Significantly Affected by 6 Gy TBI

Next, we investigated whether 6 Gy TBI resulted in altered blood urea nitrogen (BUN) and serum creatinine

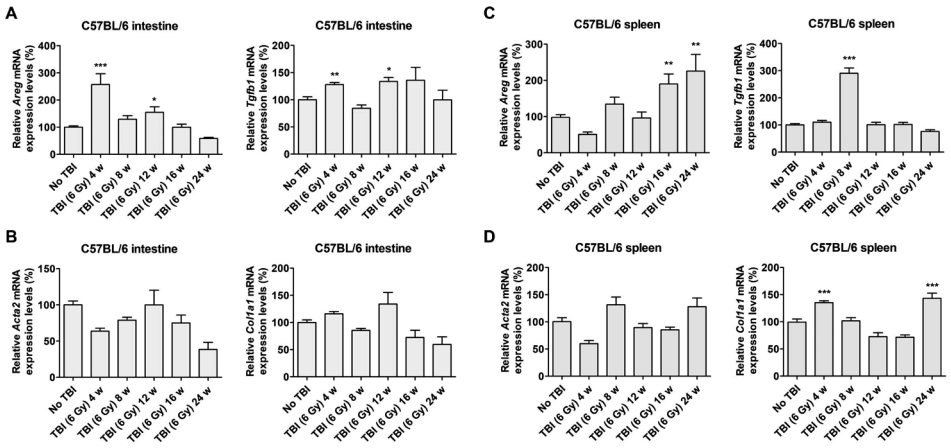

FIG. 4. Analysis of amphiregulin (AREG) signaling and fibrosis marker expression in the intestine and spleen of C57BL/6 mice in response to 6 Gy total-body irradiation (TBI). Panels A and B: Analysis of *Areg*, transforming growth factor-β1 (*Tgfb1*), α-smooth muscle actin (*Acta2*), and collagen type I alpha 1 (*Col1a1*) expression in the intestine after TBI. Panels C and D: Expression of *Areg*, *Tgfb1*, *Acta2*, and *Col1a1* mRNAs in the spleen of 6 Gy TBI model mice were confirmed by quantitative reverse transcription (qRT)-PCR. Relative expression levels were calculated for each time point, with the values obtained using non-irradiated mice set to 100. For quantifications, data (mean ± SEM) were analyzed by t-tests. $^{*}p < 0.05$, $^{**}p < 0.01$, and $^{***}p < 0.001$ compared to non-irradiated mice.

(sCr) levels in C57BL/6 mice. Increased BUN and sCr levels often indicate renal failure (*36*). We found that BUN levels were decreased by 25% in response to TBI, which slightly recovered after i.v. injection of SAMiRNA-mAREG (Supplementary Fig. S2A; https://doi.org/10.1667/RADE- 21-00220.1.S1). In contrast, neither TBI nor SAMiRNA-mAREG treatment resulted in significantly altered sCr levels (Supplementary Fig. S2B; https://doi.

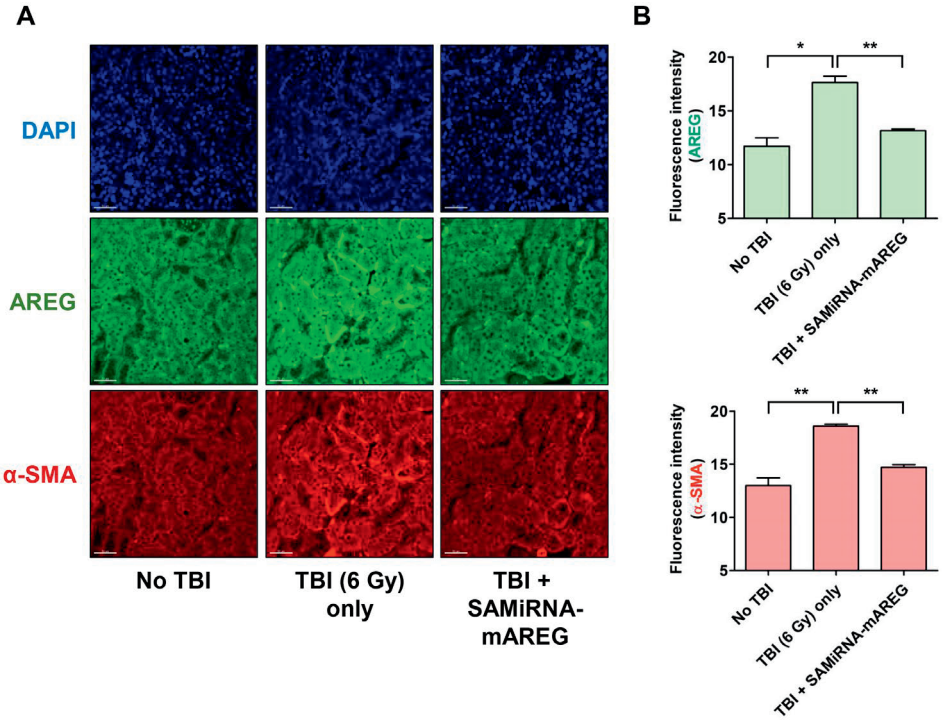

FIG. 5. Confocal microscopy images of kidney tissues isolated from mice at 24 weeks after 6 Gy total-body irradiation (TBI). Panel A: Effects of TBI and self-assembled-micelle inhibitory RNA targeting mouse amphiregulin mRNA (SAMiRNA-mAREG) treatment on AREG and α-smooth muscle actin (α-SMA) expression levels were assessed by immunofluorescence staining. The samples were co-stained for AREG (green) and α-SMA (red), as well as with DAPI to identify the nuclei (blue). Scale bar, 50 μm. Panel B: Fluorescence intensities of the signals in panel A were quantified using Fusion software. $^{*}p < 0.05$ and $^{**}p < 0.01$.

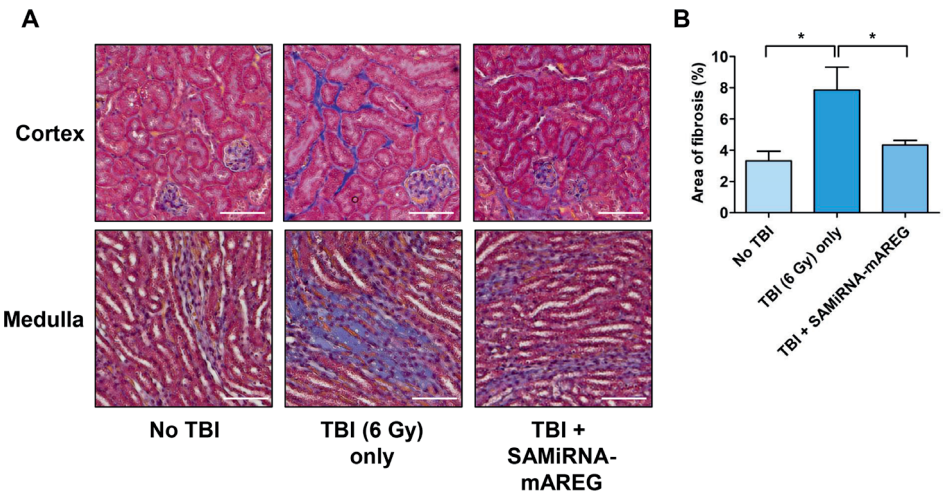

FIG. 6. Histological changes in the kidney of total-body irradiation (TBI) model mice. Panel A: Representative Masson's trichrome staining of renal cortex and medulla sections from control, TBI-only, and self-assembled-micelle inhibitory RNA targeting mouse amphiregulin mRNA (SAMiRNA-mAREG)-administered TBI mice at week 24 post-TBI. Scale bar, 100 μm. Panel B: Areas of collagen deposition were analyzed by Fiji software. $^{*}p < 0.05$.

org/10.1667/RADE- 21-00220.1.S1). These results suggest that kidney function was not significantly affected in the 6 Gy TBI mouse model.

DISCUSSION

Controlling and preventing radiation-induced side effects is important for patients receiving radiation therapy or for individuals who are subjected to occupational radiation exposure. However, the key proteins involved in radiation-induced kidney fibrosis have not been thoroughly investigated in the past. The results obtained in this study suggest that AREG is a prime candidate for inducing renal fibrosis in TBI. It was previously shown that 4 Gy TBI eliminated the ability of hematopoietic stem cells to develop into T cells in C57BL/6 mice (*10*). However, 4 Gy TBI did not cause fibrosis in any of the organs analyzed in the course of this study. We demonstrated that AREG expression was elevated in the kidneys of 6 Gy TBI mice, and renal fibrosis and inflammation were observed 24 weeks after TBI. Furthermore, our gene expression and histological analyses confirmed that i.v. injection of SAMiRNA-mAREG was able to diminish AREG and α-SMA expression, as well as collagen deposition. To the best of our knowledge, this study provides empirical evidence that downregulation of AREG expression might be an effective way to mitigate radiation-induced kidney fibrosis.

This study highlights fibrotic changes caused by 6 Gy TBI that were particularly prominent in the kidney, but absent from other organs. The comparably high-expression levels of AREG in the kidney likely triggered fibrotic signaling (AREG↑→TGF-β↑→AREG↑→…) after 6 Gy TBI. It is noteworthy that the expression of fibrotic markers, such as *Acta2* and *Col1a1* started to increase at 24 weeks after TBI, while that of *Areg* was significantly increased at all time points analyzed, i.e., 4 to 24 weeks after TBI (Fig. 2). As *Areg* expression in the kidneys of 4 Gy-irradiated mice started to increase at 8 weeks after TBI (Fig. 1A), AREG seems to be overexpressed early and in a radiation dose-dependent manner. It is thus speculated that there may be a threshold level of AREG that triggers the continuous activation of AREG signaling in response to TBI, which induces kidney fibrosis as a late effect. However, BUN and sCr levels, which reflect renal function, did not increase after 6 Gy TBI, and glomerular injury was not observed after 6 Gy TBI (Fig. 6 and Supplementary Fig. S2; https://doi.org/10.1667/RADE- 21-00220.1.S1). This could be due to the low dose applied and the short post-TBI period examined compared to other studies (*7, 10, 37*). Higher radiation doses or prolonged post-TBI periods could possibly lead to kidney malfunction.

Several previous studies revealed that the kidney is a vulnerable and radiation-sensitive abdominal organ, leading to the development of kidney disease in response to radiation (*38, 39*). It seems that kidney damage by radiation negatively affects other organs. Accordingly, protecting the kidney benefits all other organs as well. For example, atomic bomb survivors with radiation-associated chronic kidney disease are more likely to develop cardiovascular disease (*40*). Lenarczyk et al. demonstrated that WAG/RijCmcr rats receiving 10 Gy TBI with shielded kidneys showed a decrease in risk factors contributing to the development of kidney dysfunction and heart damage (*41*). In contrast, shielding of the intestines could not prevent heart disease. These results suggest that therapeutic agents that improve TBI-induced kidney damage, such as SAMiRNA-mAREG, not only protect the kidneys, but also hold the potential to prevent radiation-induced heart disease or other side effects caused by radiation.

In response to 6 Gy TBI, one out of five mice in the TBI-only and TBI with SAMiRNA-mAREG treatment groups died one week before the end of the experiment. The mice displayed approximately 30% body weight loss at the time of death compared to 4 weeks earlier. Meanwhile, the body weight of one of the four remaining mice in the TBI-only group was reduced by 20% on the day of sacrifice compared to 2 weeks earlier. Multi-organ tumorigenesis likely accounted for the significant weight loss and lethality in irradiated mice, as radiation is known to cause an accumulation of DNA damage during replication, ultimately leading to abnormal cellular signal transduction. We observed tumor-like multicellular lesions in the kidney tubules and liver veins of the TBI-only mouse with a marked decrease in body weight (Supplementary Fig. S3; https://doi.org/10.1667/RADE- 21-00220.1.S1). Additionally, a significant increase in fibrosis marker mRNA expression levels detected in this particular mouse compared to non-irradiated control mice (*Acta2*: 2.4-fold increase in the kidney and 5-fold increase in the liver; *Col1a1*: 14.5-fold increase in the kidney and 12-fold increase in the liver) led us to exclude those values in Figs. 2 and 3, as they were considered outliers. It has been demonstrated previously that AREG is involved in tumorigenesis, cancer invasion, and therapeutic resistance (*42–44*). Future studies investigating the beneficial effects of SAMiRNA-mAREG on cancer progression and survival after TBI are expected to prove useful for novel treatment strategies.

Unavoidable exposure of normal cells to radiation during radiation therapy or nuclear accidents contributes to the development of organ fibrosis. The results of this study indicate that TBI increases AREG expression in the kidney, which eventually activates fibrotic signaling. Treatment with SAMiRNA-mAREG significantly inhibited AREG and fibrosis marker expression in the kidneys. Moreover, the reduction of AREG expression led to decreased myofibroblast formation, as evidenced by the expression of α-SMA. Collectively, these findings suggest that AREG regulates the development of radiation-induced renal fibrosis. The present study provides insights into novel strategies to alleviate radiation-induced fibrosis based on SAMiRNA-mAREG-mediated downregulation of AREG expression during radiation therapy or after accidental radiation exposure.

ACKNOWLEDGMENTS

Han-Oh Park is a patent holder of SAMiRNA system. We would like to thank Editage (www.editage.co.kr) for English language editing.

Received: November 7, 2021; accepted: January 5, 2022; published online: February 11, 2022

REFERENCES

1. Bentzen SM. Preventing or reducing late side effects of radiation therapy: radiobiology meets molecular pathology. Nat Rev Cancer 2006; 6:702-13.
2. Reisz JA, Bansal N, Qian J, Zhao W, Furdui CM. Effects of ionizing radiation on biological molecules–mechanisms of damage and emerging methods of detection. Antioxid Redox Signal 2014; 21:260-92.
3. Macià IGM, Lucas Calduch A, López EC. Radiobiology of the acute radiation syndrome. Rep Pract Oncol Radiother 2011; 16:123-30.
4. López M, Martín M. Medical management of the acute radiation syndrome. Rep Pract Oncol Radiother 2011; 16:138-46.
5. Williams JP, Brown SL, Georges GE, Hauer-Jensen M, Hill RP, Huser AK, et al. Animal models for medical countermeasures to radiation exposure. Radiat Res 2010; 173:557-78.
6. Singh VK, Newman VL, Berg AN, MacVittie TJ. Animal models for acute radiation syndrome drug discovery. Expert Opin Drug Discov 2015; 10:497-517.
7. Johnston CJ, Manning C, Hernady E, Reed C, Thurston SW, Finkelstein JN, et al. Effect of total body irradiation on late lung effects: hidden dangers. Int J Radiat Biol 2011; 87:902-13.
8. DeBo RJ, Lees CJ, Dugan GO, Caudell DL, Michalson KT, Hanbury DB, et al. Late effects of total-body gamma irradiation on cardiac structure and function in male Rhesus Macaques. Radiat Res 2016; 186:55-64.
9. Kal HB, van Kempen-Harteveld ML. Renal dysfunction after total body irradiation: dose-effect relationship. Int J Radiat Oncol Biol Phys 2006; 65:1228-32.
10. Xiao S, Shterev ID, Zhang W, Young L, Shieh JH, Moore M, et al. Sublethal total body irradiation causes long-term deficits in thymus function by reducing lymphoid progenitors. J Immunol 2017; 199:2701-12.
11. Keslova P, Formankova R, Riha P, Sramkova L, Snajderova M, Malinova B, et al. Total body irradiation is a crucial risk factor for developing secondary carcinomas after allogeneic hematopoietic stem cell transplantation in childhood. Neoplasma 2020; 67:1164-9.
12. Berasain C, Avila MA. Amphiregulin. Semin Cell Dev Biol 2014; 28:31-41.
13. Harskamp LR, Gansevoort RT, van Goor H, Meijer E. The epidermal growth factor receptor pathway in chronic kidney diseases. Nat Rev Nephrol 2016; 12:496-506.
14. Zaiss DMW, Gause WC, Osborne LC, Artis D. Emerging functions of amphiregulin in orchestrating immunity, inflammation, and tissue repair. Immunity 2015; 42:216-26.
15. Arpaia N, Green JA, Moltedo B, Arvey A, Hemmers S, Yuan S, et al. A distinct function of regulatory T cells in tissue protection. Cell 2015; 162:1078-89.
16. Minutti CM, Modak RV, Macdonald F, Li F, Smyth DJ, Dorward DA, et al. A macrophage-pericyte axis directs tissue restoration via amphiregulin-induced transforming growth factor beta activation. Immunity 2019; 50:645-54.e6.
17. Lee CM, Park JW, Cho WK, Zhou Y, Han B, Yoon PO, et al. Modifiers of TGF-β1 effector function as novel therapeutic targets of pulmonary fibrosis. Korean J Intern Med 2014; 29:281-90.
18. Zaiss DMW. Amphiregulin as a driver of tissue fibrosis. Am J Transplant 2020; 20:631-2.
19. Yoon PO, Park JW, Lee CM, Kim SH, Kim HN, Ko Y, et al. Self-assembled micelle interfering RNA for effective and safe targeting of dysregulated genes in pulmonary fibrosis. J Biol Chem 2016; 291:6433-46.
20. Venkataraman T, Frieman MB. The role of epidermal growth factor receptor (EGFR) signaling in SARS coronavirus-induced pulmonary fibrosis. Antiviral Res 2017; 143:142-50.
21. Kok HM, Falke LL, Goldschmeding R, Nguyen TQ. Targeting CTGF, EGF and PDGF pathways to prevent progression of kidney disease. Nat Rev Nephrol 2014; 10:700-11.
22. Zhou Y, Lee JY, Lee CM, Cho WK, Kang MJ, Koff JL, et al. Amphiregulin, an epidermal growth factor receptor ligand, plays an essential role in the pathogenesis of transforming growth factor-

β-induced pulmonary fibrosis. J Biol Chem 2012; 287:41991-2000.

23. Shao J, Sheng H. Amphiregulin promotes intestinal epithelial regeneration: roles of intestinal subepithelial myofibroblasts. Endocrinology 2010; 151:3728-37.
24. Zamore PD. RNA interference: big applause for silencing in Stockholm. Cell 2006; 127:1083-6.
25. Akinc A, Maier MA, Manoharan M, Fitzgerald K, Jayaraman M, Barros S, et al. The Onpattro story and the clinical translation of nanomedicines containing nucleic acid-based drugs. 2019; 14:1084-7.
26. Mansoori B, Mohammadi A, Shir Jang S, Baradaran B. Mechanisms of immune system activation in mammalians by small interfering RNA (siRNA). Artif Cells Nanomed Biotechnol 2016; 44:1589-96.
27. Meng Z, Lu M. RNA Interference-Induced Innate Immunity, Off-Target Effect, or Immune Adjuvant? Front Immunol 2017; 8:331.
28. Son SS, Hwang S, Park JH, Ko Y, Yun SI, Lee JH, et al. In vivo silencing of amphiregulin by a novel effective Self-Assembled-Micelle inhibitory RNA ameliorates renal fibrosis via inhibition of EGFR signals. Sci Rep 2021; 11:2191.
29. Romesser PB, Kim AS, Jeong J, Mayle A, Dow LE, Lowe SW. Preclinical murine platform to evaluate therapeutic countermeasures against radiation-induced gastrointestinal syndrome. Proc Natl Acad Sci U S A 2019; 116:20672-8.
30. Lu Z, Ma Y, Zhang S, Liu F, Wan M, Luo J. Transforming growth factor-β1 small interfering RNA inhibits growth of human embryonic lung fibroblast HFL-I cells in vitro and defends against radiation-induced lung injury in vivo. Mol Med Rep 2015; 11:2055-61.
31. Lee JW, Tutela JP, Zoumalan RA, Thanik VD, Nguyen PD, Varjabedian L, et al. Inhibition of Smad3 expression in radiation-induced fibrosis using a novel method for topical transcutaneous gene therapy. Arch Otolaryngol Head Neck Surg 2010; 136:714-9.
32. Aryankalayil MJ, Martello S, Bylicky MA, Chopra S, May JM, Shankardass A, et al. Analysis of lncRNA-miRNA-mRNA expression pattern in heart tissue after total body radiation in a mouse model. J Transl Med 2021; 19:336.
33. Ruigrok MJR, Frijlink HW, Melgert BN, Olinga P, Hinrichs WLJ. Gene therapy strategies for idiopathic pulmonary fibrosis: recent advances, current challenges, and future directions. Mol Ther Methods Clin Dev 2021; 20:483-96.
34. Klaus R, Niyazi M, Lange-Sperandio B. Radiation-induced kidney toxicity: molecular and cellular pathogenesis. Radiat Oncol 2021; 16:43.
35. Puukila S, Lemon JA, Lees SJ, Tai TC, Boreham DR, Khaper N. Impact of ionizing radiation on the cardiovascular system: A review. Radiat Res 2017; 188:539-46.
36. Gowda S, Desai PB, Kulkarni SS, Hull VV, Math AA, Vernekar SN. Markers of renal function tests. N Am J Med Sci 2010; 2:170-3.
37. Booth C, Tudor G, Tudor J, Katz BP, MacVittie TJ. Acute gastrointestinal syndrome in high-dose irradiated mice. Health Phys 2012; 103:383-99.
38. Cohen EP. Radiation nephropathy after bone marrow transplantation. Kidney Int 2000; 58:903-18.
39. O'Donoghue J. Relevance of external beam dose-response relationships to kidney toxicity associated with radionuclide therapy. Cancer Biother Radiopharm 2004; 19:378-87.
40. Sera N, Hida A, Imaizumi M, Nakashima E, Akahoshi M. The association between chronic kidney disease and cardiovascular disease risk factors in atomic bomb survivors. Radiat Res 2013; 179:46-52.
41. Lenarczyk M, Lam V, Jensen E, Fish BL, Su J, Koprowski S, et al. Cardiac injury after 10 Gy total body irradiation: indirect role of effects on abdominal organs. Radiat Res 2013; 180:247-58.
42. Busser B, Sancey L, Brambilla E, Coll JL, Hurbin A. The multiple roles of amphiregulin in human cancer. Biochim Biophys Acta 2011; 1816:119-31.
43. Xu Q, Chiao P, Sun Y. Amphiregulin in cancer: New insights for translational medicine. Trends Cancer 2016; 2:111-3.
44. Wang S, Zhang Y, Wang Y, Ye P, Li J, Li H, et al. Amphiregulin confers regulatory t cell suppressive function and tumor invasion via the EGFR/GSK-3β/Foxp3 axis. J Biol Chem 2016; 291:21085-95.
45. Schindelin J, Arganda-Carreras I, Frise E, Kaynig V, Longair M, Pietzsch T, et al. Fiji: an open-source platform for biological-image analysis. Nat Methods 2012; 9:676-82.